

Amendment A to Global Biochar C-Sink Standard

3.2

Persistence evaluation for highly condensed biochar

Introduction of the Upper Persistence Class of Biochar

A1.1 Polycondensed aromatic structure of biochar

The principal structure of biochar consists predominantly of aromatic rings, which are structural units composed of six carbon atoms. These rings are fused into clusters, such that adjacent rings share carbon atoms along fused ring edges. Clusters of fused aromatic rings vary in size, complexity, and degree of structural organization. The biological and chemical stability of biochar increases with increasing aromaticity (i.e. the share of organic carbon bound in aromatic ring structures), increasing aromatic ring condensation (i.e. the size of fused aromatic clusters), and increasing structural ordering of aromatic domains (i.e. the three-dimensional organization and connectivity of aromatic clusters) - see Glossary A1.6.

While no biochar carbon fraction can be regarded as completely inert, increasing aromatic condensation and ordering substantially reduces the probability of biological or chemical degradation (Schmidt et al., 2025). Biochar carbon that is dominated by highly condensed aromatic structures exhibit a markedly increased likelihood of surviving for more than 1000 years after application to soil, as supported by observations of ancient charcoal and pyrogenic carbon persisting over millennial timescales in soils and sediments (Howell et al., 2022). Persistence beyond this timescale is commonly interpreted as a transition from the fast carbon cycle into the (slow) geological carbon cycle (c.f. Glossary A1.6) (Archer, 2005; Falkowski et al., 2000; Schmidt and Noack, 2000). Biochar carbon that reaches millennial persistence can therefore be considered a geological carbon sink, acknowledging

Geologically Persistent Carbon (GPC) replaces PAC terminology

In Version 3.2 of the Global Biochar C-Sink Standard, two carbon pools were defined and referred to as persistent aromatic carbon (PAC) and semi-persistent carbon (SPC). The sizes of these pools cannot be determined from biochar analysis alone and are therefore allocated using a probabilistic evaluation approach. To avoid misunderstandings arising from the chemical-analytic connotation of the term "aromatic", this amendment and the forthcoming Version 4.0 of the Standard replace PAC with the term geologically persistent carbon (GPC). GPC denotes the portion of biochar carbon that persists beyond 1000 years and thus enters the geological carbon cycle. The SPC terminology and the degradation function describing the modelled decay of this fraction over a 1000-year time horizon are retained unchanged.

that this classification reflects a probabilistic assessment of long-term stability rather than absolute permanence (see Chapter 2.2 of the Global Biochar C-Sink Standard).

A1.2 The probabilistic approach

The Global Biochar C-Sink Standard distinguishes between two conceptual carbon-sink pools based on persistence probabilities following biochar application to soil. The geological persistent carbon (GPC) pool denotes the portion of biochar carbon that persists beyond 1000 years after soil application and thus enters the geological carbon cycle. It is defined by its fate to survive the biosphere (i.e., to remain stable in the terrestrial system beyond the 1000-year threshold). The semi-persistent carbon (SPC) denotes the remaining portion that provides temporary carbon storage and returns to the rapid carbon cycle within the first 1000 years. These pools are defined by their fate over a 1000-year horizon. However, their relative sizes cannot be determined from analytical characterization alone. Long-term biochar degradation and stabilization in soil depend on complex environmental conditions such as soil mineralogy, drainage, biological activity, and climatic conditions that cannot be quantified with certainty over millennial timescales. The partitioning of biochar carbon between GPC and SPC is therefore estimated probabilistically using measurable structural proxies.

Aging of biochar in soil is not only characterized by slow biological and chemical degradation processes but also by physical and chemical stabilization mechanisms (Lehmann et al., 2024). Biochar persistence is therefore determined not only by its condensed polyaromatic structure but also by environmental factors such as the soil type and structure, its mineral content, and biological activity, temperature, rain events, pollution, slope and exposition as well as vegetation cover and land management practices¹. While all these parameters influence the probability of persistence, the condensed poly-aromatic structure of biochar is resistant to nearly everything that may happen. Moreover, with increasing residence time in soil, more biochar carbon becomes physically and chemically protected within soil particles and complexation increases. Mineral-associated stabilization may allow pyrogenic carbon to be preserved over very long timescales, even when its molecular structure is less aromatic or partly degraded (Czimczik and Masiello, 2007; Sorrenti et al., 2016).

While any fraction of biochar carbon may become physico-chemically protected in soil, the probability for a given fraction of biochar-carbon to persists for more than 1000 years increases with increasing aromatic ring condensation and structural ordering. The part of biochar that persisted 1000 years (GPC) and the part of biochar that experience degradation (SPC) consist both of a continuum of aliphatic and mostly aromatic structures with varying degrees of condensation. However, the GPC pool will contain significantly more poly-condensed structures than the SPC pool with more aliphatic and smaller

¹ It has been suggested that biochar degrades to a greater extent at higher soil temperatures in the first 100 years after soil application (Woolf et al., 2021). However, this is based mainly on laboratory studies, in which the stabilizing mechanisms can hardly come into effect. Data are simply not sufficient to quantify the temperature effect globally.

aromatic structures. GPC and SPC are not defined by chemically distinct or sharply separable fractions, but they are probabilistic pools reflecting different likelihoods of long-term persistence. To estimate the relative sizes of the GPC and SPC pools for a given biochar, analytical proxies based on measurable structural properties are required.

A1.3 Analytical proxies for biochar persistence

The degree of aromatic condensation represents an average structural property of a biochar sample that integrates a wide range of molecular configurations. It cannot be measured directly as a single physical parameter but can be approximated using several analytical proxies that correlate with the extent of aromatic ring condensation.

Historically, the molar hydrogen-to-organic-carbon ratio (H/Corg) has been the most widely used proxy to characterize the degree of aromatic condensation in biochar and to infer its relative persistence (Zimmerman and Gao, 2013). During pyrolysis, hydrogen is preferentially lost as volatile compounds, while carbon increasingly forms aromatic and polycondensed structures. As a result, decreasing H/Corg ratios generally indicate increasing aromaticity (Wiedemeier et al., 2015). This relationship has been demonstrated across a wide range of feedstocks and pyrolysis conditions and has therefore been adopted as a practical, cost-effective proxy for biochar stability (Budai et al., 2016; Woolf et al., 2021).

A key advantage of H/Corg is its empirical linkage to biochar degradation observed in pot and field experiments. Most long-term incubation, pot, and field trials that quantify biochar-derived CO₂ emissions have relied on elemental analysis as part of biochar characterization, making H/Corg the only proxy for which a substantial empirical basis exists across diverse soils, climates, and biochar types. Recent harmonized analyses and re-evaluations of biochar decomposition datasets confirm that H/Corg remains one of the most robust predictors of relative biochar persistence when evaluated against long-term mineralization data (Lehmann et al., 2024; Woolf et al., 2021). However, the analysis of H/C ratios, their correlation to other biochar parameters have some limitations (Azzi et al., 2024; Lebrun Thauront et al., 2024).

H/Corg represents an average bulk property of a biochar sample and does not resolve the internal heterogeneity of aromatic structures. In particular, it cannot sufficiently account for the influence of mineral bound H on this ratio (Hagemann et al., 2025; Sanei et al., 2025). High-ash biochars may exhibit elevated H/Corg ratios despite containing highly aromatic and polycondensed carbon structures, due mineral-bound hydrogen and catalytic interactions during pyrolysis that alter hydrogen retention without proportionally reducing aromatic condensation (Buss et al., 2019; Grafmüller et al., 2022; Lebrun Thauront et al., 2024). However, higher ash content and specifically the content of amorphous silica, may also inhibit the formation of polycondensated structures (McBeath et al., 2015). As a consequence, H/Corg may both under- and overestimate the persistence potential of ash-

rich biochars and does not reliably distinguish between different architectures of condensed aromatic clusters that may differ substantially in long-term stability.

Therefore, while H/Corg provides a conservative and empirically grounded approximation of biochar persistence, its limitations motivate the use of complementary analytical proxies that more directly capture the abundance and structural organization of highly condensed aromatic carbon fractions.

Hydropyrolysis (HyPy) has been developed as an analytical method to isolate aromatic carbon fractions with a higher degree of ring condensation in biochar by selectively removing labile and less condensed carbon compounds under high-pressure hydrogen at high temperatures. The residual carbon fraction obtained by HyPy (BC_{HyPy}) consists of aromatic clusters with more than seven condensed rings and is therefore considered a reliable approximation of the more stable biochar carbon pool (Howell et al., 2022). The carbon fraction volatilized under these extremely harsh conditions is operationally defined as the reactive carbon fraction (C_{react}) and is characterized by a substantially lower probability of surviving for more than 1000 years after application to soil.

Solid-state electric conductivity (SEC) has recently been proposed as an additional proxy for aromatic condensation, reflecting the increasing connectivity and delocalization of n -electrons in polycondensed aromatic carbon structures. SEC shows strong correlations with H/Corg and BC_{HyPy} (Hagemann et al., 2025), at least for biochars produced from the same or very similar feedstock. SEC is a relatively simple and cost-efficient method that can be measured at the production site and has the potential to complement other analytical proxies on a continuous basis (Hagemann et al., 2025).

Random reflectance (Ro) provides a detailed and robust measure of the structural ordering and maturation of aromatic carbon domains at the microscale. The mean Ro value, which has been suggested for persistence-related evaluations (Petersen et al., 2023; Sanei et al., 2025), is derived from a large number of individual point measurements across a biochar sample (typically 500 (Sanei et al., 2025)), thereby capturing its intrinsic heterogeneity. For biochar produced under constant pyrolysis conditions, the distribution of individual Ro measurements generally follows a Gaussian distribution, with the standard deviation reflecting the internal variability of aromatic condensation. Originally developed in coal petrology, Ro has been adapted for biochar analysis (Alami Sounni et al., 2026; Mastalerz et al., 2025; Sanei et al., 2025).

At each measuring point, higher reflectance values indicate a higher degree of aromatic ordering and polycondensation. Ro has been shown to correlate with pyrolysis severity, including temperature, pressure, and residence time, as well as with H/Corg ratios (with the above-discussed exceptions) and the relative abundance of more condensed aromatic carbon structures (Sanei et al., 2023, 2025). In addition, yet unpublished, datasets indicate strong correlations between Ro , SEC, and the fraction of biochar carbon resistant to hydropyrolysis, further supporting its relevance for persistence assessment.

Unlike bulk elemental proxies, Ro explicitly accounts for the coexistence of differently ordered aromatic domains within a single biochar sample, thereby providing insight into the internal distribution of more- and less-stable carbon structures. Importantly, high Ro -values do not necessarily imply chemical inertness or absolute persistence but serves as a relative indicator of the likelihood that a given fraction of biochar carbon belongs to the more condensed end of the aromatic continuum and is more likely to resist biological degradation (ICCP, 1963; Schmidt et al., 2025). In this sense, Ro supports a probabilistic interpretation of GPC and SPC pools for soil applied biochar and complements both H/Corg and HyPy by resolving structural heterogeneity that bulk and operational proxies cannot capture.

A1.4 The Upper Persistence Class of Biochar

In 2021, the Global Biochar C-Sink Standard introduced two persistence classes based on the molar hydrogen-to-organic-carbon ratio (H/Corg). Biochars with $H/Corg < 0.4$ are assigned to a persistence class in which 75% of biochar carbon is attributed to GPC (formerly known as PAC) and 25% to SPC, while biochars with $H/Corg \geq 0.4$ are assigned entirely to the SPC pool. The $H/Corg < 0.4$ threshold has been shown to be robust across a wide range of feedstocks and pyrolysis conditions. Within this framework, however, no further differentiation is made among biochars exhibiting very high degrees of aromatic ring condensation, including materials with H/Corg values well below 0.25. As a result, biochars with substantially varying degrees of aromatic condensation and structural ordering are currently grouped within the same persistence class.

Over the past years, additional analytical methods—most notably random reflectance (Ro) and hydropyrolysis (HyPy)—have generated a substantial and consistent body of data demonstrating higher discriminatory power for identifying biochars with very high degrees of aromatic condensation and structural ordering. These methods enable a more precise identification of biochars in which the reactive carbon fraction is exceptionally low and the probability of millennial-scale persistence is correspondingly high.

Based on the expanded analytical data, the present amendment introduces a third, preliminary persistence class to capture biochars at the upper end of aromatic condensation and structural ordering. This class resolves differences among highly aromatic materials with molar H/Corg ratios < 0.4 that are not captured by the existing H/Corg-based classification. For the period 2025–2026, certification of the upper persistence class is limited to a maximum of 1,000 tons of biochar that are produced and soil-applied within the “CSI – Inertinite Pilot Project”. This quantitative restriction reflects the pilot character of the new class and allows controlled implementation while additional operational experience and empirical data are gathered. Following public consultation during the first semester of 2026, the Global Biochar C-Sink Standard Version 4 is expected to formally integrate the new persistence classification.

Analyses combining Ro, HyPy, and SEC reveal a non-linear transition in biochar structure at high degrees of aromatic ring condensation. Biochars exhibiting a Mean Ro higher than 3.8% show a marked and consistent shift across multiple independent indicators. Above this threshold of 3.8%, the content of biochar carbon resistant to hydrolysis (BC_{HyPy}) consistently exceeds 90% of the total carbon. At the same time, SEC increases by more than one order of magnitude, indicating that aromatic cluster connectivity has progressed to a level at which biochar transitions from an electrical insulator to a semi-conductor (publication of SEC data pending). These converging changes indicate that aromatic domains are no longer merely larger, but qualitatively more ordered and interconnected.

The transition observed around a Mean Ro value of 3.8% reflects a structural inflection point rather than a gradual progression. Beyond this point, further increases in pyrolysis severity lead to only minor changes in reactivity, while increased ordering and connectivity dominate material behavior. The Mean Ro threshold of 3.8% represents a conservative, empirically derived boundary at which biochar carbon shifts into a regime characterized by exceptionally low reactivity and a very high probability of millennial-scale persistence. This regime corresponds approximately to molar H/Corg ratios below 0.25, as independently observed in recent datasets (Hagemann et al., 2025; Sanei et al., 2025, 2024).

The Upper Persistence Class of Biochar

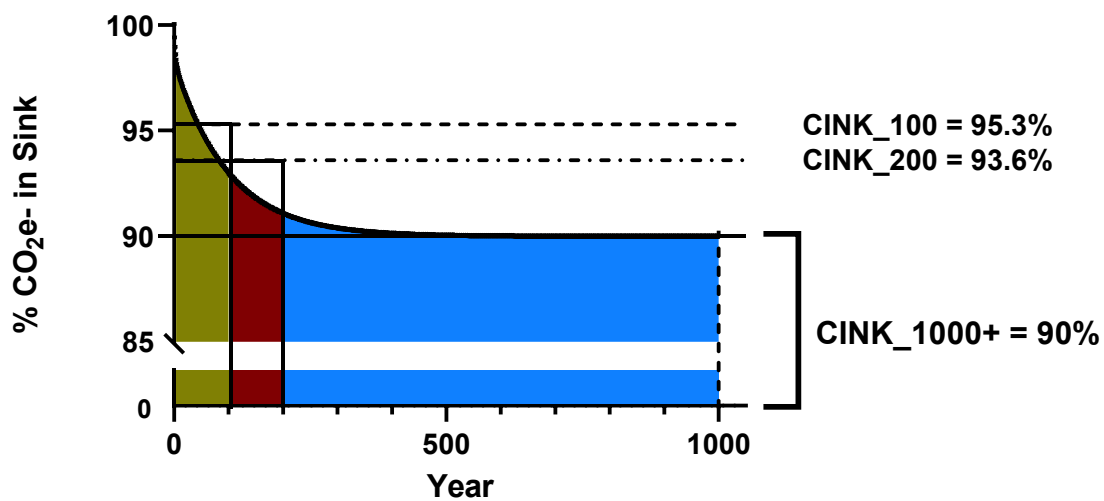


Figure A1 Schematic illustration of the partitioning of biochar carbon into geologically persistent carbon (GPC) and semi-persistent carbon (SPC). Biochars meeting the new upper persistence class, GPC is conservatively set to 90% of total organic carbon and treated as a stable pool persisting beyond 1000 years, representing transfer into the geological carbon cycle. The remaining 10% is assigned to SPC and follows an exponential degradation function as defined for the SPC pools in the Biochar C-Sink Standard. The figure illustrates the persistence allocation and the conservative separation between long-term geological storage (GPC) and modeled degradation (SPC), rather than spatial or chemical gradients within the biochar material. CINK_H refers to the average annual C-sink potential over H years and is calculated with the equations provided in the standard.

Biochars are assigned to the new upper persistence class if they meet at least one of the following criteria:

- (i) a mean random reflectance of $Ro \geq 3.8\%$, while no more than 3% of all measured points present $Ro < 2\%$ and the ≥ 500 Ro measured points present a Gaussian distribution with a heterogeneity score ≤ 8 .
- (ii) a fraction of biochar carbon resistant to hydropyrolysis exceeding 90%.

For biochars assigned to this upper persistence class, 90% of total biochar carbon are assigned to the GPC pool and 10% to the SPC pool. The allocation corresponds to a conservative lower-bound probability of long-term persistence, since such biochars typically exhibit less than 10% reactive carbon. Accordingly, the probability that biochar carbon within this class persists for more than 1000 years after application to soil can be conservatively considered to be at least 90%.

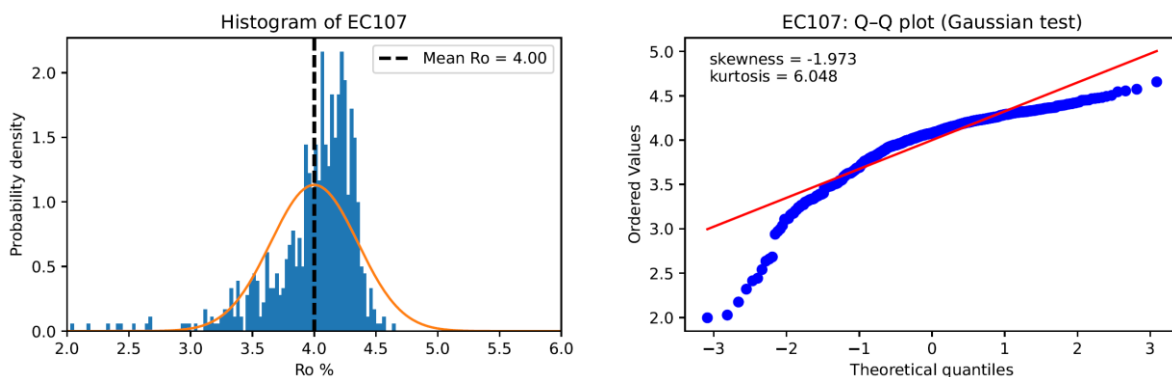


Figure A2 A total of $n = 687$ Ro measurements were available, with $n = 686$ classified as IBRo. The full-sample mean Ro was 4.00%, and the cleaned mean was 4.04% after excluding 24 outliers (3.49%) using a median absolute deviation (MAD) modified Z-score threshold. The molar H to C ratio of the sample is 0.17. A fixed 5th 95th percentile trim retained $n = 617$ and gave a trimmed mean of 4.03%. Central quantiles were tightly clustered, with the 25th/50th/75th percentiles at 3.88%, 4.08%, and 4.23%. The 5th and 95th percentiles were 3.34% and 4.36%, indicating a relatively narrow central spread with limited tail extension on this scale. Skewness was -1.97, which is consistent with mild left-skewness, and excess kurtosis was 6.05, indicating heavier tails than a Gaussian reference. The histogram contains multiple local maxima (peak count = 3), indicating a more complex distributional shape; this peak count alone does not establish multimodality. The Q-Q relationship shows clear departures from linearity, with $qq-r^2 = 0.84$ as the squared correlation coefficient of the Q-Q fit. Lower-tail deviations exceed upper-tail deviations based on the mean absolute error (MAE) in the tails. The CDF-based Cramér von Mises deviation was $CvM(*1000) = 6.31$, suggesting elevated global scatter relative to a Gaussian reference across the full distribution. Maximum reflection, defined as the mean Ro of the highest 20 measurements after outlier cleaning, was 4.48%, giving a maximum-reflection-to-mean ratio (maximum reflection / mean cleaned) of 1.11. Heterogeneity score = 5.00, driven mainly by increased global distributional scatter relative to a Gaussian reference, as reflected by the CDF-based Cramér von Mises deviation, and clear departures from Q Q linearity. Overall, the dataset shows some irregularities but seems still suitable for reporting.

Ro and HyPy are strongly related to aromatic condensation, but differ in analytical nature, availability, and operational constraints. Random reflectance resolves microscale heterogeneity and is particularly effective at detecting mixed biochars and unstable pyrolysis conditions, whereas hydropyrolysis isolates an operationally defined carbon fraction associated with higher ring condensation. When investigating biochar sets produced systematically under increasing pyrolysis severity from different feedstocks, both methods indicated the same structural transitions and showed consistent agreement with other persistence-relevant indicators such as H/Corg and SEC. Accepting either criterion, therefore, preserves scientific robustness while enabling practical

implementation across different production and laboratory settings. The allocation of 90% of total carbon to the GPC pool is conservative regardless of whether classification is based on Ro or HyPy.

Biochars with a mean Ro below 3.8% and/or more than 3% of measuring points $\leq 2\%$ (IBRo), and molar H/Corg below 0.4 remain eligible for registration under the existing H/Corg-based persistence classification, with 75% allocated to the GPC pool and 25% to the SPC pool. The method will be further refined in the next standard update (i.e., Version 3.2 to 4.0), introducing, probably, more than these two persistence classes.

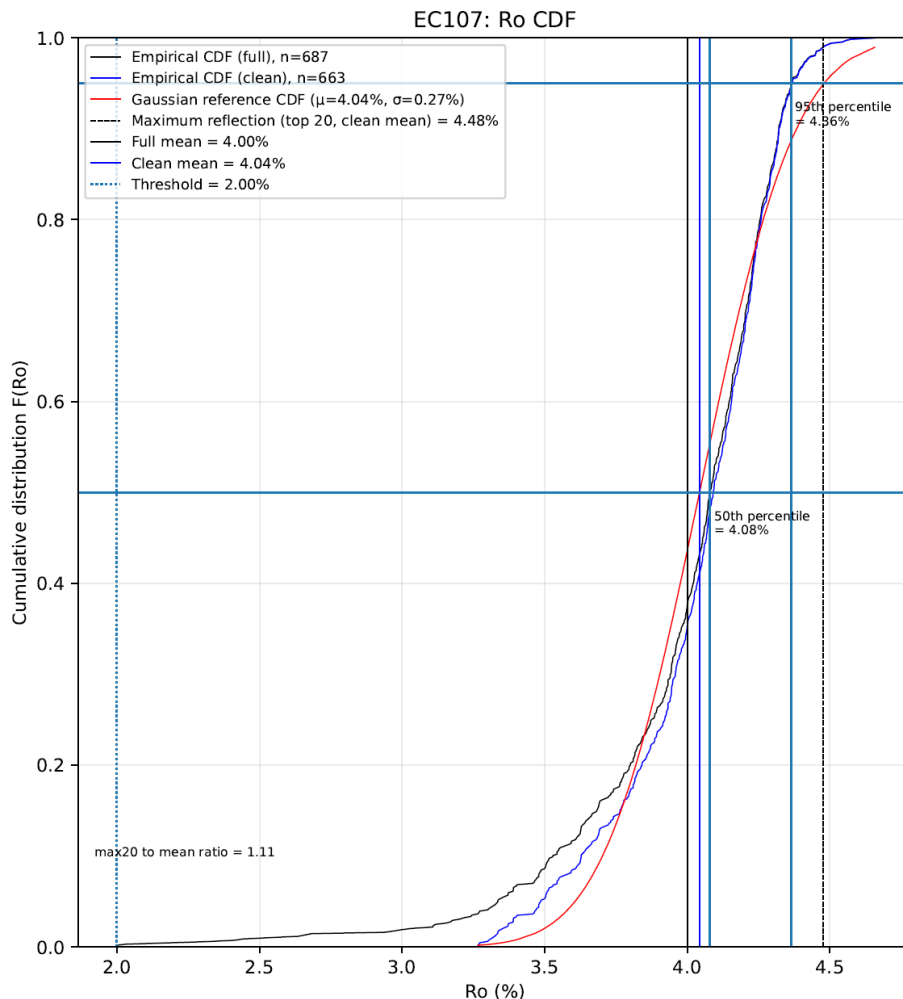


Figure A3 The cumulative distribution function (CDF) panel shows the empirical Ro distribution as cumulative probability versus Ro. It summarizes the full dataset ($n = 687$) and the outlier-cleaned subset ($n = 663$) for comparison. A Gaussian reference curve is included as a descriptive benchmark using the sample μ and σ , and should not be interpreted as evidence of normality. Vertical annotations highlight central tendency estimates and the maximum reflection marker where shown.

A1.5 Sampling, shipping, laboratory endorsement

Samples for Ro and/or HyPy analyses must be submitted as part of the CSI registered batch sample to an EBC-endorsed laboratory. Separate sampling is not permitted. The EBC-endorsed laboratory shall take a subsample under controlled conditions and forward it to a CSI-endorsed laboratory for Ro and/or HyPy analysis. For the pilot certification

(limited to a total amount of 1000 t biochar), direct shipping of representative samples to Fusinite Ltd, London, may exceptionally be accepted.

A1.6 Glossary for the Amendment

1000-year threshold

Carbon in soil that survived 1000 years is considered as having entered the geological carbon cycle. However, the distinction between the fast and geological carbon cycles is conceptual rather than absolute; the 1000-year threshold represents a policy-relevant boundary at which carbon storage is treated as geological, acknowledging that carbon-cycle processes operate along a continuum of timescales.

Aromatization, aromatic ring condensation, and structural ordering of aromatic domains describe complementary aspects of biochar carbon speciation that emerge concurrently with increasing pyrolysis severity, while differing in their sensitivity to specific process parameters and analytical proxies. The definitions of the four principal terms are outlined below.

Aromatization (aromaticity increase)

The conversion of non-aromatic carbon structures (aliphatic, oxygenated and other compounds) in biomass into aromatic carbon domains during pyrolysis. Increasing aromatization is typically reflected by decreasing molar H/Corg (and typically O/Corg) ratios. More aromatization results in purer aromatic carbon rings with fewer hydrogen, oxygen, and other heteroatom-containing functional groups at the edges of the aromatic structures.

Aromatic ring condensation (extend of ring fusion)

The progressive fusion of aromatic rings into larger clusters (polycondensation) and the shift toward larger polycyclic aromatic structures composed of an increasing number of fused rings. Higher aromatic ring condensation corresponds to larger polycyclic aromatic domains and is associated with reduced chemical and biological reactivity.

Hydropyrolysis (HyPy) operationally isolates a carbon fraction dominated by highly condensed aromatic clusters (commonly comprising more than seven fused rings), thereby distinguishing it from less condensed aromatic structures. Random reflectance (Ro) increases with increasing aromatic ring condensation and reflects the growth and maturation of fused aromatic domains.

Fast Carbon Cycle

The part of the global carbon cycle involving the exchange of carbon among the atmosphere, biosphere, soils, and oceans through biological, chemical, and physical processes operating on timescales from years to centuries and extending up to millennial timescales. Carbon within the fast carbon cycle remains part of the climate-relevant surface Earth system and may return to the atmosphere on policy-relevant timescales.

Geological Carbon Cycle

Carbon storage and transfer through geological processes operating over millennial to geological timescales, including burial, sedimentation, mineralization, volcanic activity, and tectonic recycling.

Pyrolysis severity

The combined thermal and chemical forcing of biomass during the pyrolysis process, determined by process parameters such as temperature, heating rate, residence time of gas and solid pyrolysis products, and gas pressure or atmosphere in the reactor.

Pyrolysis severity governs the extent to which biochar carbon undergoes the following chemical and structural transformation. Applying the same pyrolysis intensity to two types of biomass can result in biochars with different reactivity. Not only different carbon structures of the feedstock, but also catalytic effects of mineral components affect biochar reactivity and its poly-condensed structure.

Structural ordering of aromatic domains

The increased ordering and maturation of aromatic carbon domains (fused aromatic clusters) with rising pyrolysis severity. Structural ordering includes greater alignment, stacking, and connectivity of polycondensed aromatic structures and enhanced π -electron delocalization. It reflects a transition from disordered aromatic clusters toward more ordered, graphitic-like arrangements and is captured by proxies such as random reflectance and solid-state electrical conductivity.

Alami Sounni, K., Camps-Arbestain, M., Kaal, J., Tighe, C.J., Titirici, M.M., Siavalas, G., 2026. Assessment and integration of different methodologies for the characterisation of carbon aromaticity and structure in biochar. *Int. J. Coal Geol.* 313, 104925. <https://doi.org/10.1016/J.COAL.2025.104925>

Archer, D., 2005. Fate of fossil fuel CO₂ in geologic time. *J. Geophys. Res. Oceans* 110, 1–6. <https://doi.org/10.1029/2004JC002625>;WGROU:STRING:PUBLICATION

Azzi, E.S., Li, H., Cederlund, H., Karlstun, E., Sundberg, C., 2024. Modelling biochar long-term carbon storage in soil with harmonized analysis of decomposition data. *Geoderma* 441, 116761. <https://doi.org/10.1016/J.GEODERMA.2023.116761>

Budai, A., Rasse, D.P., Lagomarsino, A., Lerch, T.Z., Paruch, L., 2016. Biochar persistence, priming and microbial responses to pyrolysis temperature series. *Biol. Fertil. Soils* 52, 749–761. <https://doi.org/10.1007/S00374-016-1116-6/FIGURES/5>

Buss, W., Jansson, S., Mašek, O., 2019. Unexplored potential of novel biochar-ash composites for use as organo-mineral fertilizers. *J. Clean. Prod.* 208, 960–967. <https://doi.org/10.1016/J.JCLEPRO.2018.10.189>

Czimczik, C.I., Masiello, C.A., 2007. Controls on black carbon storage in soils. *Global Biogeochem. Cycles* 21. <https://doi.org/10.1029/2006GB002798>

Falkowski, P., Scholes, R.J., Boyle, E., Canadell, J., Canfield, D., Elser, J., Gruber, N., Hibbard, K., Hogberg, P., Linder, S., Mackenzie, F.T., Moore, B., Pedersen, T., Rosenthal, Y., Seitzinger, S., Smetacek, V., Steffen, W., 2000. The global carbon cycle: A test of our knowledge of earth as a system. *Science* (1979). 290, 291–296. <https://doi.org/10.1126/SCIENCE.290.5490.291>;WEBSITE:WEBSITE:AAAS-SITE;JOURNAL:JOURNAL:SCIENCE;WGROU:STRING:PUBLICATION

Grafmüller, J., Böhm, A., Zhuang, Y., Spahr, S., Müller, P., Otto, T.N., Bucheli, T.D., Leifeld, J., Giger, R., Tobler, M., Schmidt, H.P., Dahmen, N., Hagemann, N., 2022. Wood Ash as an Additive in Biomass Pyrolysis: Effects on Biochar Yield, Properties, and Agricultural Performance. *ACS Sustain. Chem. Eng.* 10, 2720–2729. https://doi.org/10.1021/ACSSUSCHEMENG.1C07694/ASSET/IMAGES/LARGE/SC1C07694_M003.JPG

Hagemann, N., Schmidt, H.P., Bucheli, T.D., Grafmüller, J., Vossinkel, S., Herdegen, V., Meredith, W., Uguna, C.N., Snape, C.E., 2025. Proxies for use in biochar decay models: Hydropyrolysis, electric conductivity, and H/C_{org} molar ratio. *PLoS One* 20, e0330206. <https://doi.org/10.1371/JOURNAL.PONE.0330206>

Howell, A., Helmkamp, S., Belmont, E., 2022. Stable polycyclic aromatic carbon (SPAC) formation in wildfire chars and engineered biochars. *Science of The Total Environment* 849, 157610. <https://doi.org/10.1016/J.SCITOTENV.2022.157610>

ICCP, 1963. International handbook of coal petrography. International handbook of coal petrography 1–232.

Lebrun Thauront, J., Soja, G., Schmidt, H.P., Abiven, S., 2024. A critical re-analysis of biochar properties prediction from production parameters and elemental analysis. *GCB Bioenergy* 16, e13170. <https://doi.org/10.1111/GCBB.13170>

Lehmann, J., Abiven, S., Azzi, E., Fang, Y., Singh, B.P., Sohi, S., Sundberg, C., Woolf, D., Zimmerman, A.R., 2024. Persistence of biochar: Mechanisms, measurements, predictions. *Biochar for Environmental Management: Science, Technology and Implementation* 277–311. <https://doi.org/10.4324/9781003297673-11/PERSISTENCE-BIOCHAR-JOHANNES-LEHMANN-SAMUEL-ABIVEN-ELIAS-AZZI-YUNYING-FANG-BHUPINDER-PAL-SINGH-SARAN-SOHI-CECILIA-SUNDBERG-DOMINIC-WOOLF-ANDREW-ZIMMERMAN>

Mastalerz, M., Drobniak, A., Liu, B., Sauer, P.E., 2025. Reflectance as an indicator of biochar permanence. *Int. J. Coal Geol.* 306, 104809. <https://doi.org/10.1016/J.COAL.2025.104809>

McBeath, A. V., Wurster, C.M., Bird, M.I., 2015. Influence of feedstock properties and pyrolysis conditions on biochar carbon stability as determined by hydrogen pyrolysis. *Biomass Bioenergy* 73, 155–173. <https://doi.org/10.1016/J.BIOMBIOE.2014.12.022>

Petersen, H.I., Lassen, L., Rudra, A., Nguyen, L.X., Do, P.T.M., Sanei, H., 2023. Carbon stability and morphotype composition of biochars from feedstocks in the Mekong Delta, Vietnam. *Int. J. Coal Geol.* 271, 104233. <https://doi.org/10.1016/J.COAL.2023.104233>

Sanei, H., Rudra, A., Przyswitt, Z.M.M., Kouston, S., Sindlev, M.B., Zheng, X., Nielsen, S.B., Petersen, H.I., 2024. Assessing biochar's permanence: An inertinite benchmark. *Int. J. Coal Geol.* 281, 104409. <https://doi.org/10.1016/J.COAL.2023.104409>

Sanei, H., Wojtaszek-Kalaitzidi, M., Schovsbo, N.H., Stenshøj, R., Zhou, Z., Schmidt, H.-P., Hagemann, N., Chiaramonti, D., Kiaitsis, T., Rudra, A., Lehner, A.J., Brown, R.W., Gill, S., Dorr, E., Kalaitzidis, S., Goodarzi, F., Petersen, H.I., 2025. Quantifying inertinite carbon in biochar. *Int. J. Coal Geol.* 310, 104886. <https://doi.org/10.1016/J.COAL.2025.104886>

Schmidt, H.-P., Abiven, S., Cowie, A., Glaser, B., Joseph, S., Kammann, C., Lehmann, J., Leifeld, J., Pan, G., Rasse, D., Rumpel, C., Woolf, D., Zimmerman, A.R., Hagemann, N., 2025. Biochar Permanence—A Policy Commentary. *GCB Bioenergy* 17, e70092. <https://doi.org/10.1111/GCBB.70092>;PAGE:STRING:ARTICLE/CHAPTER

Schmidt, M.W.I., Noack, A.G., 2000. Black carbon in soils and sediments: Analysis, distribution, implications, and current challenges. *Global Biogeochem. Cycles* 14, 777–793. <https://doi.org/10.1029/1999GB001208>

Sorrenti, G., Masiello, C.A., Dugan, B., Toselli, M., 2016. Biochar physico-chemical properties as affected by environmental exposure. *Science of the Total Environment* 563–564, 237–246. <https://doi.org/10.1016/j.scitotenv.2016.03.245>

Wiedemeier, D.B., Abiven, S., Hockaday, W.C., Keiluweit, M., Kleber, M., Masiello, C.A., McBeath, A. V., Nico, P.S., Pyle, L.A., Schneider, M.P.W., Smernik, R.J., Wiesenberg, G.L.B., Schmidt, M.W.I., 2015. Aromaticity and degree of aromatic condensation of char. *Org. Geochem.* 78. <https://doi.org/10.1016/j.orggeochem.2014.10.002>

Woolf, D., Lehmann, J., Ogle, S., Kishimoto-Mo, A.W., McConkey, B., Baldock, J., 2021. Greenhouse Gas Inventory Model for Biochar Additions to Soil. *Environ. Sci. Technol.* 55, 14795–14805. <https://doi.org/10.1021/ACS.EST.1C02425>

Zimmerman, A.R., Gao, B., 2013. The Stability of Biochar in the Environment, in: Ladygina, N., Rineau, F. (Eds.), Biochar and Soil Biota. Boca Raton, pp. 1–40.